Available online at www.sciencedirect.com
SCIENCE DIRECT®
Polymer 45 (2004) 3923–3932
polymer
www.elsevier.com/locate/polymer

Effects of chain stiffness and penetrant size on penetrant diffusion in simple polymers: deduced relations from simulation and PRISM theory

Joanne Budzien[a], John D. McCoy[a,*], Dana Rottach[b], John G. Curro[c]

[a]*Department of Materials and Metallurgical Engineering, New Mexico Institute of Mining and Technology, Socorro, NM 87801, USA*
[b]*Department of Chemical and Nuclear Engineering, University of New Mexico, Albuquerque NM 87131, USA*
[c]*Sandia National Laboratories, Albuquerque, NM 87185, USA*

Received 30 May 2003; received in revised form 13 December 2003; accepted 13 December 2003

Abstract

Molecular dynamics simulations in the NVT ensemble were performed for a repulsive system of bead-spring polymer chains with angle constraints. The diffusion coefficients of spherical penetrants were measured for different size penetrants as the angle constraints were varied. The scaling of the diffusion coefficient with penetrant size varies as a function of chain stiffness from liquid-like behavior to polymeric behavior. Free volume distributions were calculated from both simulation and PRISM theory. It is found that free volume distributions and mean void size are constant with chain stiffness although the diffusion coefficient changes by a factor of two. This suggests that while free volume is necessary for diffusion to occur, binary collisions and chain relaxation also play a role in determining penetrant diffusion. The relative contributions of these factors to the diffusion coefficient may change as a function of chain stiffness.

Keywords: Penetrant; PRISM theory; Stokes–Einstein relation

1. Introduction

Correlating dynamic properties with molecular structure is an active area of research. Certainly, few people would argue that structure should affect dynamic quantities such as viscosity, diffusion, and the glass transition temperature. Whether dynamic properties can be entirely predicted from knowledge of the underlying structure and thermodynamics is still unknown. In this work, we consider the effect of chain stiffness, penetrant diameter and free volume distribution on the diffusion of small molecule penetrants in polymers.

Simple models are capable of capturing much of the pertinent physics. A well-studied simple polymer model is the semi-flexible chain model of Kremer and Grest [1]. In this model, the polymer is stripped to the essential physics. Polymers are modeled as chains of connected sites with excluded volume interactions and small fluctuations about a well-defined bond length. To study penetrants, one only needs add unconnected sites. This work extends [2] and corrects [3] previous research on this polymer-penetrant system and focuses on correlations between the penetrant and the polymer properties.

To obtain the structure, one can use simulation, experiment, or theory. A theory that has been successful in describing polymer structure is the Polymer Reference Interaction Site Model (PRISM) theory [4]. PRISM theory relates the intramolecular and intermolecular structure through a single integral equation, which can be solved either self-consistently or using prior knowledge of the intramolecular structure. The benefit of using theory over simulation is the speed at which results can be obtained, especially as the model of interest becomes more complicated.

Historically, there have been several ways to correlate diffusion coefficients with the surrounding medium. Probably, the most widely used as a first approximation is the Stokes–Einstein relation. The Stokes–Einstein relation is often invoked even for situations in which few of the underlying assumptions are valid and works surprisingly well. In cases for which the Stokes–Einstein relation fails, it is common to make empirical corrections based on a data

* Corresponding author. Tel.: +1-505-835-5379; fax: +1-505-835-5625.
E-mail address: mccoy@mailhost.nmt.edu (J.D. McCoy).

0032-3861/$ - see front matter © 2004 Elsevier Ltd. All rights reserved.
doi:10.1016/j.polymer.2003.12.084

set. These corrections are generally applicable to only a small class of substances.

In the polymer community, free volume is the concept often invoked to correlate diffusion coefficients with polymer properties. Recent experimental work has involved positron annihilation lifetime spectroscopy to determine free volume [5,6]. Recent studies of small molecule diffusion in polymers (using both simulated and experimental data) have looked at the connection between free volume and diffusivity with varying degrees of success [7–9].

In this work, it is seen that the effect of penetrant size on the diffusion coefficient is modified depending on chain flexibility. From the free volume distribution and mean void size, it is shown that this result is not due to a change in free volume; the free volume distribution is essentially constant as chain stiffness varies. Rather, it appears that chain mobility itself is the source of this effect. As the chain stiffness increases, the number of sites on the polymer that must have coordinated motions increases. This changes the local dynamics and the relative effects of system relaxation, binary collisions, and free volume that a penetrant experiences.

2. Simulation and theory details

2.1. Theory of diffusion

The study of diffusion in liquids is a multifaceted field with a long history. Many theories and correlations have been proposed for diffusion in liquids and specifically in alkanes. Some of these correlations have a theoretical basis with empirically fit parameters [10] and others are purely empirical fits [11,12] assuming that the diffusion coefficient should be a function of system variables such as size, temperature, or density. Since, the focus in the current work is the effects of penetrant size and chain flexibility on the penetrant diffusion coefficient, only a few predictive equations are of interest here. This section gives some brief descriptions of the equations to which the results of this paper will be compared.

It is instructive to make use of the Stokes–Einstein analysis at the continuum level. The Einstein relation

$$D = \frac{k_B T}{\zeta} \tag{1}$$

shows that the diffusion coefficient of the solute (D) is inversely proportional to the solute friction coefficient (ζ) and proportional to temperature (T). If the friction coefficient can be described using Stokes law, the result is the Stokes–Einstein relation

$$D = \frac{k_B T}{6\pi R_s \eta} \tag{2}$$

where R_s is the hydrodynamic radius of the solute and η is the viscosity of the solvent. This relation is used with fair results even for instances where the conditions for Stokes law are inapplicable.

A commonly used correlation based on the Stokes–Einstein relation is due to Wilke and Chang [13]. It allows for a different penetrant size dependence determined from experimental data:

$$D = a\frac{TM_c^{1/2}}{\eta_c d_s^{1.8}} \tag{3}$$

where a is a constant dependent on system type, d is a molecular diameter extracted from the molal volume at the normal boiling point (assuming spherical molecules), and M is the molecular weight. For consistency throughout this paper, subscript s refers to a solute property and subscript c refers to a solvent property. A modification to the Wilke–Chang relation suggested for use with a wider range of solvents [14] is due to Scheibl. It has behavior that changes based upon relative penetrant size. For small solutes, it is simply the Stokes–Einstein equation with an additional multiplicative constant. For large solutes ($d_s \geq 1.4d_c$), the equations reduce to

$$\frac{D\eta_c}{T} = \text{constant}\left(\frac{1}{d_s} + \frac{3^{2/3}d_c^2}{d_s^3}\right) \tag{4}$$

Instead of modifying Stokes law empirically, mode-coupling theory allows a more molecular basis for the calculation of the friction coefficient ζ [15]. The basic premise is that there are two parts to the friction coefficient: one due to the binary collisions between the solvent and the solute and one due to the multiple correlated collisions due to high density and/or attractions. The idea specific to mode-coupling theory is the method by which the correlated collisions are related to the solvent properties. Since the equations to be solved using mode-coupling theory are not explicitly a function of penetrant size, there is no need to consider them further here.

However, it is not necessary to use the continuum level Einstein equation as a starting point. Enskog theory [16] can be used to calculate the diffusion coefficient using a molecular basis. This theory is based on binary collisions determining the diffusion coefficient. For a dense mixture of hard spheres, the diffusion coefficient can be calculated from [17]

$$D = \frac{3}{8nd_{sc}^2 g_{sc}(d_{sc})}\left(\frac{(m_s + m_c)k_B T}{2\pi m_s m_c}\right)^{1/2} \tag{5}$$

where n is the total number density, d_{sc} is the arithmetic average of the hard sphere diameters, m_x is the mass of component x (x = c or s), and $g_{sc}(d_{sc})$ is the unlike pair correlation function. Using a modification of the Percus–Yevick equation of state for hard spheres, one can calculate

g_{sc} from [17,18]

$$g_{sc}(d_{sc}) = \frac{d_s g_{cc}(d_{sc}) + d_c g_{ss}(d_{sc})}{2d_{sc}} \tag{6}$$

where

$$g_{ii} = \frac{1}{1-x} + \frac{3y_i}{2(1-x)^2} + \frac{y_i^2}{2(1-x)^3} \tag{7}$$

$$x_i = \frac{\pi n_i d_i^3}{6} \tag{8}$$

$$x = x_i + x_j \tag{9}$$

$$y_i = \frac{d_j x_i + d_i x_j}{d_j} \tag{10}$$

with i and j taking the values of s or c as appropriate. Modifications exist so that Eq. (5) can be used for systems other than hard spheres and at high density. A standard modification is the assumption of rough hard spheres [19]. This modification entails multiplying the Enskog diffusion coefficient by a system dependent constant. This constant corrects for the correlated collisions due to higher density and the conversion of translational motion into rotational motion in polyatomic systems. The dependence of this constant on system variables such as size of the molecules, deviation from spherical molecules, temperature, density, and type of molecular interactions has been the subject of multiple papers [17,20–24] with no clear consensus reached.

In these small-molecule theories, the size of the solvent is based on a spherical model with an effective radius of gyration. However, for long chain molecule solvents with a small species as the solute (e.g. methane in tetracosane), the radius of gyration may be an inappropriate measure of relative sizes.

Free-volume theory [25] is a traditional means to calculate the diffusion coefficient of penetrants in polymers

$$D = A \exp\left[-\frac{B\hat{V}}{V_0} \right] \tag{11}$$

where A and B are constants for a particular system, V_0 is a free volume, and $\hat{V}$ is a characteristic volume of the solute. There has been a substantial amount of effort as evidenced by the literature to make Eq. (11) amenable to calculations based upon readily available solute and polymer properties. Thus far, there has been no overwhelmingly successful method to do this.

For organic systems, Bosma and Wesslingh [26] combined the Stokes–Einstein equation with the free volume equation to get

$$D = \frac{k_B T}{3\pi \eta_c d_s}\left[1 + b\sqrt{\frac{d_c \rho_c}{d_s \rho_s}} \exp\left(-\frac{\gamma}{v_{free,c}}\left(\frac{d_s}{d_c} - 1 \right) \right) \right] \tag{12}$$

where $v_{free,c}$ is the free volume of the solvent divided by its closest packed volume, ρ is density, and γ is a constant of 0.8.

2.2. Simulation details

The systems studied here have five penetrants and 16 chains each of length 50 sites or five penetrants in a solvent of 800 sites for atomic systems. Molecular dynamics simulations were performed [27] in the NVT ensemble using a velocity Verlet algorithm. The temperatures were set equal to one in reduced Lennard–Jones units using a Nosé–Hoover [28] thermostat with a frequency constant of 0.1 inverse time units (1.0 for atomic systems). The reduced number density of sites was constant at 0.84 in a volume of $958.33\sigma^3$. There was a variation in packing fraction of about 2% from 0.46 to 0.47. The time step size was 0.006. Systems were equilibrated for at least 10^6 time steps with production runs of 7×10^6 time steps.

Simulations were performed using the standard purely repulsive, semi-flexible chain model [1]. The potential for the bonded atoms is

$$\begin{aligned} U_{bond}(r) &= -0.5HR_0^2 \ln\left[1 - \left(\frac{r}{R_0} \right)^2 \right] & r < R_0 \\ U_{bond}(r) &= \infty & \text{otherwise} \end{aligned} \tag{13}$$

Following previous work [1,2], $H = 30$, $R_0 = 1.5$. The stiffness of the chain was varied using a harmonic potential [2]

$$U_{stiff}(\theta) = K(\theta - \theta_0)^2 \tag{14}$$

with $K = 0$, 1, 5, 10, 20, 100, and 500 in Lennard–Jones energy units and $\theta_0 = 2\pi/3$.

In addition, there is a purely repulsive Lennard–Jones interaction between all sites in the model [2]:

$$\begin{aligned} U_{\alpha\beta}(r) &= 4\varepsilon\left[\left(\frac{\sigma}{r - \Delta_{\alpha\beta}} \right)^{-12} - \left(\frac{\sigma}{r - \Delta_{\alpha\beta}} \right)^{-6} + \frac{1}{4} \right] & r \le 2^{1/6}\sigma + \Delta_{\alpha\beta} \\ U_{\alpha\beta}(r) &= 0 & \text{otherwise} \end{aligned} \tag{15}$$

where α and β denote the identity of the sites involved (type c or s). Both σ and ε were assigned values of unity in these simulations. The $\Delta_{\alpha\beta}$ indicates a shift due to different size penetrants. The polymer sites always interact with $\Delta_{cc} = 0$. Cross-interactions are calculated using the arithmetic mean. Simulations were performed with different size penetrants in the polymer. The mass of every site was set equal to one even for the varying size penetrants. Penetrant sizes reported here have been

normalized so that polymer sites have a diameter $d_c = 1.0$.

For this system with $K = 0$, the entanglement length has been reported as between 32 and 110 sites [1] so the current chain length of 50 sites is within this range. However, the entanglement effects are not expected to be important for the penetrant diffusion analysis performed in this work. To calculate the diffusion coefficient of the penetrant from simulation, one can use the penetrant motion and the Einstein relation

$$\langle|\vec{R}(t) - \vec{R}(0)|^2\rangle = 6Dt \tag{16}$$

where R is the position of a penetrant, t is time, and D is the diffusion coefficient. The angle brackets denote an average over equivalent sites and all starting positions. This equation is valid only at long times. In this work, diffusion coefficients were extracted from simulation through the equation

$$D = \frac{1}{6}\frac{\mathrm{d}\langle R^2\rangle}{\mathrm{d}t} \tag{17}$$

It is equivalent to the Einstein relation at long times. The time region to be fit was determined from a plot of $\log\langle R^2\rangle$ versus log time for times at which the slope is unity.

2.3. PRISM theory

The average intramolecular structure for α and γ type sites on a single chain can be written as

$$\hat{\Omega}_{\alpha\gamma}(k) = \frac{1}{N_\alpha}\sum_{i\in\alpha}\sum_{j\in\gamma}\left\langle\frac{\sin kr_{ij}}{kr_{ij}}\right\rangle \tag{18}$$

where k is the wave vector, r_{ij} is the distance between sites i and j, and N_α is the number of sites of type α. The sums are over all sites of a given type. This intermolecular structure is characterized by the pair correlation functions $g_{\alpha\gamma}$ or equivalently by

$$h_{\alpha\gamma}(r) = g_{\alpha\gamma}(r) - 1. \tag{19}$$

The generalized Ornstein–Zernike equation [29] relates the two structure types through the direct correlation function $C_{\alpha\gamma}(r)$. In matrix notation in Fourier space, this becomes

$$\hat{h}(k) = \hat{\Omega}(k)\hat{C}(k)[\hat{\Omega}(k) + \rho\hat{h}(k)] \tag{20}$$

where ρ is the number density. To solve this equation, one needs a closure relation for the direct correlation function. It has been found for liquid-like densities that the Percus–Yevick relation is appropriate [4,29]. For a hard core potential, the Percus–Yevick closure can be written as

$$\begin{aligned} g_{\alpha\gamma}(r) &= 0 \quad \text{for } r < d_{\alpha\gamma} \\ C_{\alpha\gamma}(r) &= 0 \quad \text{for } r > d_{\alpha\gamma} \end{aligned} \tag{21}$$

It has been demonstrated [4] that PRISM theory is most compatible with repulsive potentials. Using the repulsive potential defined for the simulation ($U_{\alpha\beta}(r)$ from Eq. (15)), this $d_{\alpha\gamma}$ can be calculated from the Barker–Henderson equation

$$d = \int_0^\infty \left(1 - \exp\left[-\frac{U(r)}{k_B T}\right]\right)\mathrm{d}r \tag{22}$$

It has also been demonstrated [30] that PRISM theory predicts a greater compressibility for polymer melts than is seen experimentally. This can be corrected through a modified Percus–Yevick closure for the polymer sites

$$\begin{aligned} g_{pp}(r) &= 0 \quad \text{for } r < d_{pp} \\ C_{pp}(r) &= C_{HC}(d_{pp})\left[\frac{d_{pp}}{r}\right]^a \quad \text{for } r > d_{pp} \end{aligned} \tag{23}$$

where $C_{HC}(d_{pp})$ is the hard core $C(r)$ at contact and a is a constant chosen to match the PRISM isothermal compressibility to experimental values. A value of $a = 15$ works reasonably well for the models considered here.

2.4. Free volume

To calculate the free volume from PRISM theory, one calculates the reversible work of growing a spherical cavity, which is related to the insertion probability and then to the free volume distribution. The work of inserting a spherical void of radius R (denoted $w(R)$) can be written as

$$\frac{w(R)}{k_B T} = \pi R\rho\sum_\alpha \int_0^1 \mathrm{d}\lambda\left[d_\alpha + 2\lambda R\right]^2 g_{\alpha d}^{(\lambda)}\left(\frac{d_\alpha + \lambda 2R}{2}\right) \tag{24}$$

where $g_{\alpha d}^{(\lambda)}$ is the value at contact and λ is a charging parameter that varies the size of the void from a point ($\lambda = 0$) to a full size void of radius $R(\lambda = 1)$. To calculate the pair correlation function for a polymer-void at contact, one uses the PRISM Eq. (20) with the single chain structure taken from the simulation and either closure Eq. (21) or (23). For a spherical cavity, the intramolecular structure factor is unity for all k and the cross-term is zero.

This reversible work is related to the insertion probability as

$$P(R) = f_0 \exp\left[-\frac{w(R)}{k_B T}\right] \tag{25}$$

where f_0 is the free volume fraction or, equivalently, one minus the packing fraction. The insertion probability also can be written [31] as

$$P(R) = \int_R^\infty f(r)\mathrm{d}(r) \tag{26}$$

where $f(r)$ is the free volume distribution. By taking the derivative of Eq. (26), one can calculate $f(r)$ numerically. It is useful to define an average void size, $\langle R\rangle$, and distribution width by $\langle R^2\rangle - \langle R\rangle^2$, where the average is defined in the

customary way through the distribution function

$$\langle R^n \rangle = \int_0^\infty R^n f(R) \mathrm{d}R \tag{27}$$

The reversible work of insertion can also be calculated from scaled particle theory [32,33]. For point particles ($r \leq d_p/2$), the work of insertion can be written as [32]

$$W(r) = -k_B T \ln\left(1 - \frac{4}{3}\pi r^3 \rho\right) \tag{28}$$

where $W(R)$ differs from $w(R)$ due to the method of incorporating the base free volume afforded by the packing fraction. For very large voids, the work can be written as [32]

$$W(r) = \frac{4}{3}\pi r^3 \Pi + 4\pi r^2 S_0 \tag{29}$$

where Π is the pressure and S_0 is an interfacial tension between a hollow, rigid sphere and the polymer sites. To interpolate between the two limits, an expansion in radius is used [32]

$$W(r) = a_0 + a_1 r + a_2 r^2 + a_3 r^3 \tag{30}$$

The expansion coefficients are determined through using the large (Eq. (29)) and small (Eq. (28) for $r = d_p/2$) limits. They are [32]

$$\begin{aligned} a_0 &= k_B T\left\{\ln\left(\frac{1}{1-y}\right) + \frac{9}{2}X^2\right\} - \frac{\pi d_c^3}{6}\Pi, \\ a_1 &= -\frac{k_B T}{d_c}\{6X + 18X^2\} + \pi d_c^2 \Pi, \\ a_2 &= \frac{k_B T}{d_c^2}\{12X + 18X^2\} - 2\pi d_c \Pi, \qquad a_3 = \frac{4}{3}\pi\Pi \end{aligned} \tag{31}$$

where $y = \pi d_c^3 \rho/6$ is the packing fraction and $X = y/1 - y$. Eqs. (30) and (31) can be used in conjunction with Eq. (25) (the f_0 term is already included in the a_0 term for scaled particle theory) to calculate the insertion probability.

In addition, the insertion probabilities and free volume distributions can be calculated directly from simulation. Polymer configurations are saved periodically. A fine grid is superposed on the configuration. At each grid point, a sphere is inserted and grown until it overlaps a polymer site. Statistics are kept about the maximum inserted test sphere sizes achieved.

Table 1
Diffusion coefficients (σ^2/t_0) for purely repulsive penetrants in FENE repulsive LJ chains. Sizes have been normalized so that a polymer site diameter is 1.0

Penetrant size	Atomic system	$K = 0$	$K = 10$	$K = 100$	$K = 500$
0.8	0.092	0.075	0.057	0.035	0.032
1.0	0.067	0.046	0.030	0.014	0.012
1.2	0.047	0.032	0.017	0.008	0.007
1.5	0.032	0.016	0.007	0.003	0.002

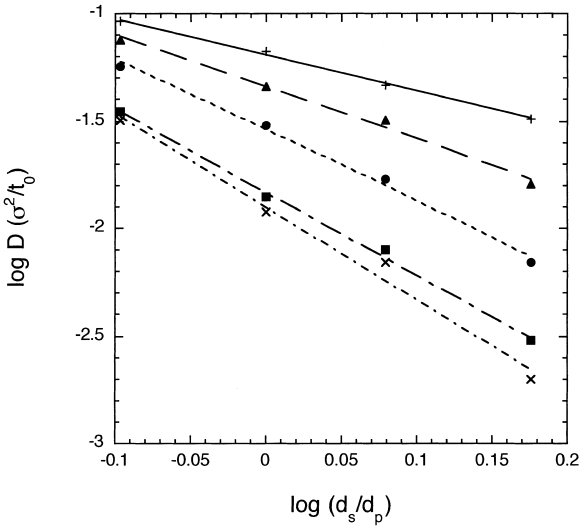

Fig. 1. Diffusion coefficient as a function of penetrant size and chain stiffness. Atomic systems (pluses), $K = 0$ (triangles), $K = 10$ (circles), $K = 100$ (squares), $K = 500$ (x's). Lines are best fits.

3. Results

3.1. Diffusion coefficients

The diffusion coefficients for a range of penetrant sizes from 0.8 to 1.5 (in polymer site units) in atomic solvents and chains of varying stiffnesses are plotted in Fig. 1. The data for these systems are in Table 1 and the slopes extracted from Fig. 1 are given in Table 2. It can be seen that, as one would expect, the diffusion coefficient decreases with increasing penetrant size in the same solvent. As chain stiffness increases, penetrant diffusion decreases and the dependence of the diffusion coefficient on penetrant size becomes a more negative power.

To gauge the reasonableness of the size dependence, we can compare with theory and correlation. The atomic system slope of -1.7 is consistent with Wilke–Chang correlation [13] (Eq. (3) predicts a value of -1.8) and is not very different from the -1.5 expected from Enskog theory using Eq. (5) (see Fig. 2). The penetrants simply are not large enough for the Stokes–Einstein relation (slope $= -1$) to apply (some literature estimates [15,26] are that size ratios of 2–3 are necessary). None of the chain systems are particularly close to the alkane predictions, although the

Table 2
The power dependence of diffusion coefficient on penetrant size as a function of chain stiffness

Chain stiffness K	Slope from log–log plot
Atomic	−1.7
0	−2.4
10	−3.3
100	−3.8
500	−4.3

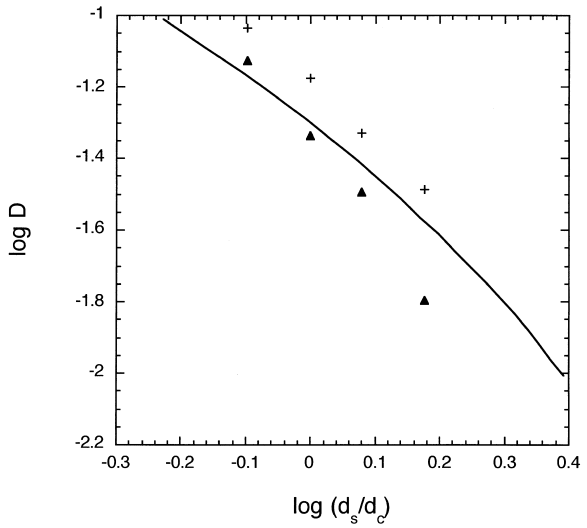

Fig. 2. Comparison of simulated results and Enskog theory. Eq. (5) (line), atomic systems (pluses), $K = 0$ (triangles).

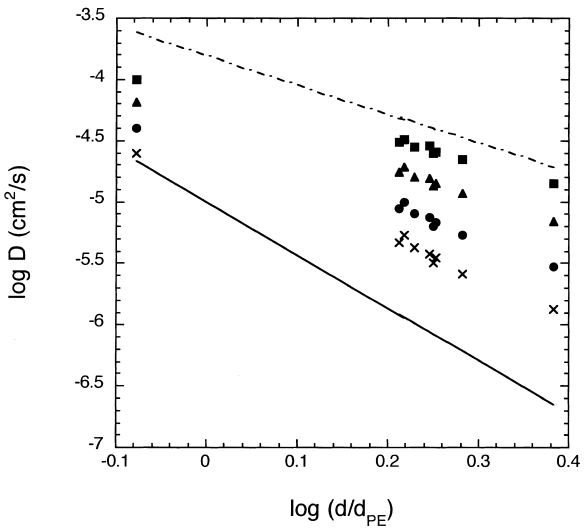

Fig. 3. Diffusion coefficient of molecules in alkanes using data from Refs. [34,35]. Hexane (squares), nonane (triangles), tridecane (circles), hexadecane (x's), slope for $K = 0$ (dot dashed line), slope for $K = 500$ (solid line). The $K = 0$ and $K = 500$ lines have arbitrary offsets along the log D axis.

Steibl correlation (Eq. (4)) with a slope of -3 is closest for the $K = 10$ case of -3.3.

Some of this lack of agreement may be due to the assumptions behind the theories and correlations that are inapplicable in this case. One unmet assumption is that though the current systems contain chain and solvent molecules, they are not truly alkane-solute systems due to the lack of attractions. The simulation model has been shown to adequately describe the melt behavior of polymer chains [1]; nonetheless, the interaction between solvent and solute may not be properly captured. This may make some difference although it is expected for dense systems that the repulsive interactions are dominant in determining diffusion [19].

Another difficulty is that the theories are based on non-penetrating spheres as both solvent and solute. While the individual sites of a chain may act as spheres, the entire chain is not a sphere and chains freely interpenetrate. The empirically determined correlations and modifications to the theories do not explicitly include this connected, non-sphericality. Thus, while the correlations may well describe the experimental alkane systems, the reported size dependence may not be the 'correct' size dependence because it is compensating for other factors such as attractions, non-spherical penetrants, and a change in mass with penetrant size.

Since the correlations and theories have some difficulties associated with them, we have reanalyzed some experimental data specifically for the size dependence. A recently reported set of experiments [34,35] used a series of rather large aromatic hydrocarbon penetrants (biphenyl, anthracene, diphenylacetylene, diphenylbutadiyne, pyrene, perylene, coronene, rubrene) and oxygen in the homologous series hexane through hexadecane to determine deviations from the Stokes–Einstein relation. Using these results including the values for the penetrant size (based on an equivalent sphere diameter), a plot similar to Fig. 1 was made for each alkane. Fig. 3 shows a few examples. To normalize the penetrant size with respect to the solvent, the value of $d_{\text{solvent}} = 4.013$ Å was used. This value was calculated from the van der Waals volume [36] for polyethylene repeat units (C_2H_4).

It can be seen that as chain length increases, slope becomes more negative. The figure also shows that by choosing what range of penetrant sizes are of interest, the slope of the log D–log d plot changes. However, in all cases, the slope becomes more negative as solvent chain length increases. Since our focus is on polymers, the long chain limit of the slope is of interest. The slope versus reciprocal chain length was plotted and the linear region was fit for a few penetrant size ranges. Table 3 has some representative data for these ranges. The infinite chain length values range from -3.2 to -6.7. This accords well with the $K = 10$, 100 and 500 values of -3.3 to -4.3. The $K = 0$ case with a slope of -2.4 falls as expected between the atomic case and a chain with additional restrictions. It is still less than the cubic dependence from naïve free volume considerations and greater than the -2 from a simple binary collision argument.

3.2. Free volume

The void insertion probability for a range of void sizes was calculated from PRISM theory and configurations saved from MD simulation for a chain stiffness $K = 0$. The results are shown in Fig. 4. It can be seen that the two methods give similar results for small free volume sizes. The inset emphasizes the larger size voids. It can be seen here that, due to the over-estimation of polymer compressibility, PRISM predicts a larger insertion probability than is seen in simulation.

Table 3
The size dependence of diffusion coefficients in alkanes from the slope in a log D–log(d/d_{PE}) plot

Alkane	All solutes	Small solutes[a]	All solutes except rubrene	All solutes except oxygen	All solutes except oxygen and rubrene
Hexane	−1.82	−1.68	−1.70	−2.04	−2.24
Heptane	−1.92	−1.80	−1.88	−2.18	−2.47
Octane	−2.05	−1.90	−1.99	−2.37	−2.76
Nonane	−2.09	−1.94	−2.03	−2.44	−2.86
Decane	−2.17	−2.00	−2.10	−2.56	−3.05
Undecane	−2.24	−2.05	−2.17	−2.66	−3.21
Dodecane	−2.37	−2.11	−2.29	−2.86	−3.51
Tridecane	−2.42	−2.14	−2.34	−2.93	−3.62
Tetradecane	−2.57	−2.25	−2.47	−3.14	−3.95
Pentadecane	−2.64	−2.30	−2.54	−3.25	−4.12
Hexadecane	−2.73	−2.37	−2.62	−3.38	−4.32
Long chain extrapolation	−3.8	−3.2	−3.6	−4.7	−6.7

[a] $0.83 < (d/d_{PE}) < 1.7$.

Applying the correction for compressibility to PRISM does improve agreement with simulation results as can be seen in the inset of Fig. 4.

The results for the probability of insertion calculated from simulation, scaled particle theory, and PRISM theory are compared in Fig. 5. Simulation and scaled particle theory are in good agreement, while PRISM theory has a slightly greater probability of finding a large void. The discrepancy between the simulation and scaled particle theory at large void sizes may be in part due to the size of the error in the pressure extracted from simulation.

The calculated free volume distribution for the chain stiffness $K = 0$ is plotted in Fig. 6. The shape of the curve at very small void radii is sensitive to the numerical uncertainties in taking the derivative of the insertion probability and the maximum shown may be a result of numerical error. The agreement between theory and simulation is reasonable, and, as was seen with insertion probability, correcting PRISM theory for compressibility leads to better agreement for large void radii as is seen in the inset to the figure.

Calculations were performed for chains with stiffness parameters $K = 0$ to 20. There are significant differences in the intermolecular and intramolecular structures with variation in K as can be seen in Figs. 7 and 8. However, very little difference is seen in the insertion probability or free volume distribution. Averages from both simulation and theory are listed in Table 4. These results show that there is little dependence of free volume distribution or average void size on chain stiffness. This result is consistent with previous simulation results [37,38]. In those simulations, it was found that, at constant free volume fraction, changing the chain flexibility through the torsion potential, the equilibrium bond angle, or different main chain groups affected the penetrant diffusion coefficient. Chains with greater flexibility are associated with a larger diffusion coefficient.

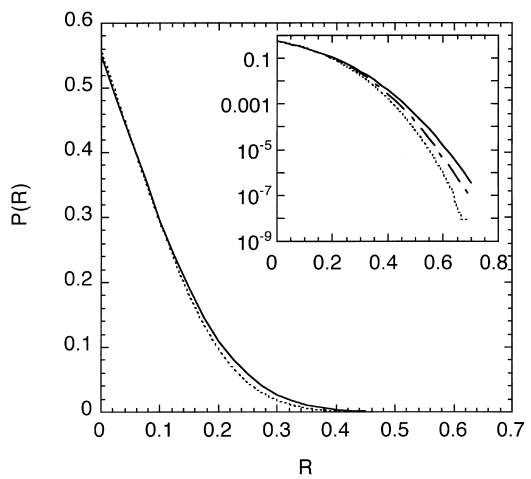

Fig. 4. Insertion probability for a semi-flexible chain liquid with chain stiffness $K = 0$. Solid curve is PRISM theory; dotted curve is MD simulation. Inset is log $P(R)$ versus R. The dot-dashed line is the PRISM with compressibility correction.

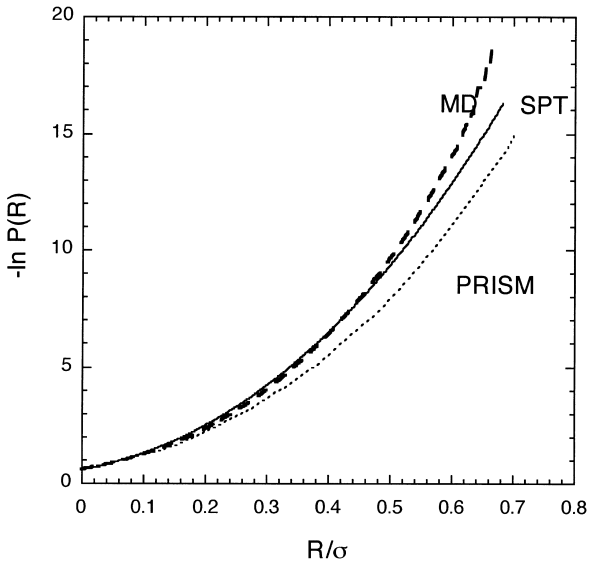

Fig. 5. Probability of finding a void of radius R or larger in tangent-sphere chains. MD is simulation result; SPT is scaled particle theory result; PRISM is polymer reference interaction site model theory result.

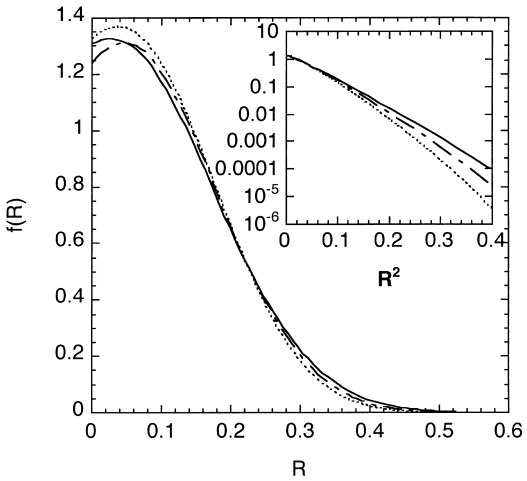

Fig. 6. Free volume distribution for a semi-flexible chain liquid with chain stiffness $K = 0$. Solid curve is PRISM theory, dotted curve is MD simulation, and dot-dashed curve is from PRISM theory with compressibility correction. The inset is a plot of $\log f(R)$ versus R^2.

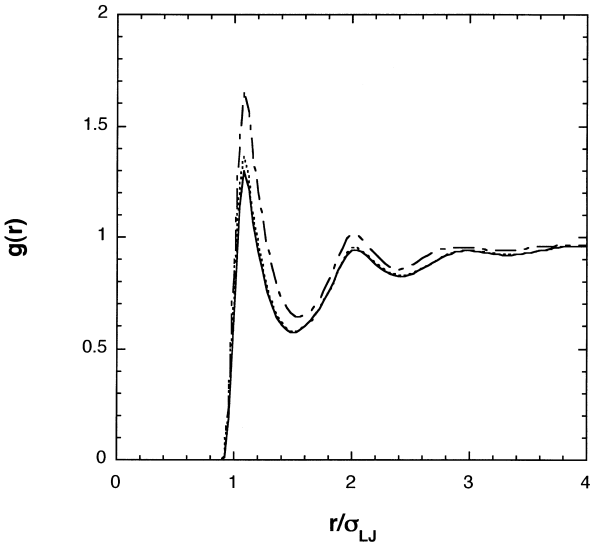

Fig. 8. Intermolecular pair correlation function for semi-flexible chains. Dot-dashed line is $K = 20$, dotted line is $K = 1$, solid line is $K = 0$.

4. Discussion

While free volume is necessary for diffusion to occur, knowing the static free volume distribution is not sufficient to predict diffusion. It has been well established that the polymer mobility has a significant effect on the penetrant diffusion coefficient. It has been found in simulations [39–42] that penetrants in rigid polymer matrices will not diffuse unless the free volume is connected. In addition, it has been shown [43] that while a 'jumping' motion may be employed by the penetrant, the free volume concentration near the penetrant need not change during this jump. Instead, it is sufficient for the polymer to move and allow two voids to become connected.

There are instances in the literature where it has been mentioned in passing that it is not necessarily the amount of free volume present, but also the shape of the voids [44] and their change in shape with time [6,7,43] that determine penetrant diffusion coefficient. Our results are consistent with these ideas. While, we have considered explicitly only free volume of spherical shape, the free volume probabilities were calculated for very small voids. Although, we do not know how these small voids are connected, the fact that the size dependence of the penetrant diffusion coefficient changes with chain flexibility seems to indicate that the time behavior of the connectivity is altered even if the shape or distribution of free volume is not. This result is also consistent with previous simulation results [45] in which it was found that diffusion coefficient was influenced in a complicated manner by polymer mobility.

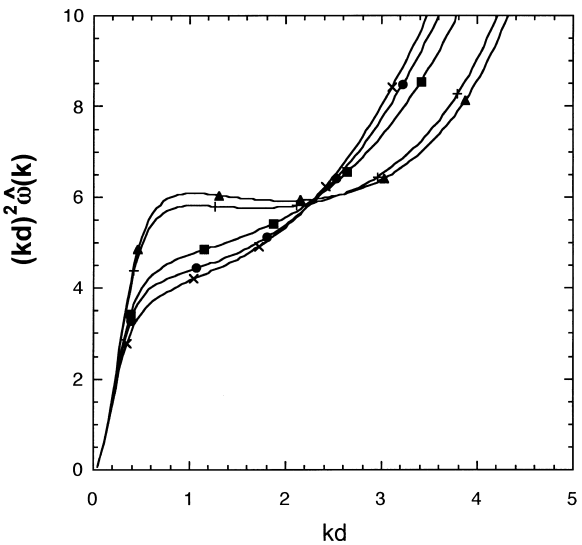

Fig. 7. Kratky plot of the single chain structure factor of semi-flexible chains obtained from MD simulations with various chain stiffnesses. $K = 0$ (triangles), 1 (pluses), 5 (squares), 10 (circles), 20 (x's).

The current trend in obtaining theoretical predictions for diffusion is to combine multiple theories and examine the relative contributions to the diffusion coefficient. Following Bosma and Wesslingh [26], the relative contributions to the diffusion coefficient change as the penetrant size changes. The two dominant terms from Eq. (12) (assuming equal densities, $\gamma = 0.8$, and $v_{\text{free,c}} = 0.3$) are plotted in Fig. 9. It can be seen that the free volume term dominates at small

Table 4
Average free volume in units of d (for a packing fraction of 0.45 and a site density of 0.85)

Polymer	PRISM	MD	Π from MD
$K = 0\langle R\rangle$	0.123	0.119	4.7 ± 0.3
$K = 0\langle R^2\rangle - \langle R\rangle^2$	0.00768	0.00714	
$K = 1\langle R\rangle$	0.125	0.119	4.8 ± 0.3
$K = 1\langle R^2\rangle - \langle \mathrm{R}\rangle^2$	0.00827	0.00706	
$K = 5\langle R\rangle$	0.1258	0.119	4.9 ± 0.3
$K = 5\langle R^2\rangle - \langle R\rangle^2$	0.00818	0.00704	
$K = 20\langle R\rangle$	0.1263	0.120	4.7 ± 0.5
$K = 20\langle R^2\rangle - \langle R\rangle^2$	0.00823	0.00717	

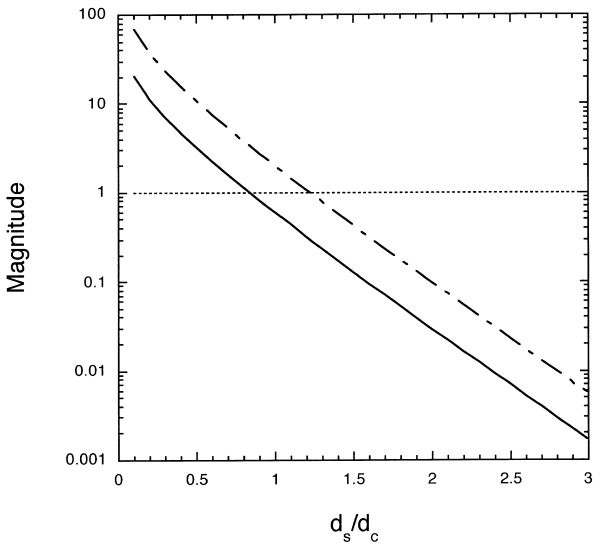

Fig. 9. Relative contribution to diffusion from free volume and hydrodynamics from Eq. (12). Plotted is $\frac{3\pi\eta_c d_s D}{k_B T}$ versus size for hydrodynamics (dotted line), free volume $b = 0.6$ (solid line), free volume $b = 2.0$ (dot-dashed line).

penetrant size and that the Stokes–Einstein term dominates at large penetrant size. In between is a region in which both terms have nearly equal magnitude. This would seem to indicate that both ideas should be incorporated.

A similar effect was seen using a mode-coupling approach [15]. For large solutes, hydrodynamics (the Stokes–Einstein relation) was important. As solute size decreased, the binary collisions and density relaxations determined the diffusion coefficient. At small penetrant size, only the binary collisions were necessary. For equally sized solute and solvent, the binary collisions were already contributing more than half of the friction coefficient. For a combination simulation and experimental study of a large (relative to site size) penetrant in different length alkanes [46], it was found that friction coefficient varied with chain length. The postulated explanation was a crossover regime as chain length increased so that there was a segmental friction coefficient rather than the whole chain contributing.

These ideas can be applied to our results as well. For the atomic case, each site is able to move based on the collisions it experiences and the space available. This space available may not be free volume in the standard sense of the term. Although all masses are equal, from geometric packing considerations, larger sites may be able to push smaller sites out of the way.

Upon linking sites into chains with no angle constraints, the chain sites not only lose mobility due to the connectivity, but also the direction in which an individual chain site can move is restricted because part of its surroundings will always be blocked by its bonded neighbors. Since the vast majority of the sites are chain sites with these new restrictions, the entire system dynamics slow. From a strict kinetic theory view, assuming that the system corrections cancel and that the proper mass of the polymer is that of the whole chain, the ratio of the interdiffusion coefficients for the solute in a chain system and an atomic system should be $1/\sqrt{2}$. This works well for the $K = 0$ systems for penetrants about the same size as a polymer site and is an overestimate as K increases.

As the angle constraint is applied, the connectivity restriction on motion becomes greater as the second bonded neighbors must also move so that a chain site can move. The motion of any site is now more dependent on a chain segmental motion or system relaxation and the relative effect of the collisions is likely to be lessened. Since the dependence on penetrant size is different for these means of transport, the size dependence of the diffusion coefficient is likely to change. This is consistent with the results in Table 3 where the size dependence of the diffusion coefficient varied as a function of relative penetrant size considered.

5. Conclusions

Molecular dynamics simulations of a semi-flexible chain polymer with penetrants were performed to determine the diffusion coefficient as a function of penetrant size and polymer flexibility. It was found that the size dependence of the penetrant diffusion coefficient varies regularly with chain flexibility from the near liquid-like behavior of penetrant diameter raised to the -2.4 power to a more chain-like behavior with an exponent of -4.3. None of the systems exhibited the Stokes–Einstein limit of penetrant diameter to the -1 power.

PRISM theory and simulation were both used to determine free volume distribution and free volume size. There was good agreement between the two methods in the average void size and size distribution width. While the polymer structure varied as chain flexibility varied, there was not a similar variance in the free volume distribution or in the average void size. The free volume was constant across all chain stiffnesses.

It was hypothesized that the change in penetrant size dependence of the diffusion coefficient may be a result of the change in dynamics of the system due to increasing stiffness. As stiffness increases, the group nature of the chain sites' motions becomes more apparent. These concerted motions may affect the local dynamics so that there is a change in relative contributions to the penetrant diffusion coefficient from collision-driven dynamics, system relaxation, and free volume. Since these mechanisms have different penetrant size dependencies, the overall diffusion coefficient size dependence will change as the relative contributions change.

References

[1] Grest GS, Kremer K. Phys Rev A 1986;33:3628. Kremer K, Grest GS. Phys Rev Lett 1988;61:566. Kremer K, Grest GS. J Chem Phys 1990; 92:5057.

[2] Rottach DR, Tillman PA, McCoy JD, Plimpton SJ, Curro JG. J Chem Phys 1999;111:9822.
[3] There was an error in the simulations for Ref. [2]. The reported diffusion coefficients are incorrect for values of K less than or equal to 10. The values reported here are from simulations without that error.
[4] Schweizer KS, Curro JG. Adv Polym Sci 1994;116:321. Schweizer KS, Curro JG. Adv Chem Phys 1997;98:1.
[5] Kobayashi Y, Zheng W, Meyer EF, McGervey JD, Jamieson AM, Simha R. Macromolecules 1989;22:2302.
[6] Dammert RM, Maunu SL, Maurer FHJ, Neelov IM, Niemelä S, Sundholm F, Wästlund C. Macromolecules 1999;32:1930.
[7] Nagel C, Schmidtke E, Günther-Schade K, Hofmann D, Fritsch D, Strunskus T, Faupel F. Macromolecules 2000;33:2242.
[8] Tanaka K, Kawai T, Kita H, Okamoto K, Ito Y. Macromolecules 2000;33:5513.
[9] Tonge MP, Gilbert RG. Polymer 2001;42:1393.
[10] Zhu Y, Lu X, Zhou J, Wang Y, Shi J. Fluid Phase Equilib 2002;194-197:1141.
[11] Wong CF, Hayduk W. Can J Chem Engng 1990;68:849.
[12] Siddiqi MA, Lucas K. Can J Chem Engng 1986;64:839.
[13] Wilke CR, Chang P. AIChE J 1955;1:264.
[14] Reid RC, Prausnitz JM, Sherwood TK. The properties of gases and liquids, 3rd ed. New York: McGraw-Hill; 1977.
[15] Bhattacharyya S, Bagchi B. J Chem Phys 1997;106:1757.
[16] Chapman S, Cowling TG. The mathematical theory of non-uniform gases, 3rd ed. London: Cambridge University Press; 1970. p. 258.
[17] Alder BJ, Alley WE, Dymond JH. J Chem Phys 1974;61:1415.
[18] Mansoori GA, Carnahan NF, Starling KE, Leland TW. J Chem Phys 1971;54:1523.
[19] Chandler D. J Chem Phys 1975;62:1358.
[20] Matthews MA, Akgerman A. J Chem Phys 1987;87:2285.
[21] Dymond JH. Chem Soc Rev 1985;14:317.
[22] Ruckenstein E, Liu H. Ind Eng Chem Res 1997;36:3927.
[23] Erkey C, Rodden JB, Akgerman A. Can J Chem Engng 1990;68:661.
[24] Speedy RJ, Prielmeier FX, Varday T, Lang EW, Ludemann HD. Mol Phys 1989;66:577.
[25] Cohen MH, Turnbull D. J Chem Phys 1959;31:1164.
[26] Bosma JC, Wesselingh JA. Trans Inst Chem Engng 1999;77A:325.
[27] LAMMPS Ver. 4.0 licensed from Sandia National Laboratories, Plimpton SJ. J Comp Phys 1995;117:1.
[28] Hoover WG. Phys Rev A 1985;A31:1695. Nosé S. Mol Phys 1984;52:255.
[29] Hansen JP, McDonald IR. Theory of simple liquids, 2nd ed. London: Academic Press Ltd; 1990.
[30] Curro JG, Webb EB, Grest GS, Weinhold JD, Pütz M, McCoy JD. J Chem Phys 1999;111:9073.
[31] Reiss H, Hammerich AD. J Phys Chem 1986;90:6252.
[32] Reiss H, Frisch HL, Helfand E, Lebowitz JL. J Chem Phys 1960;32:119.
[33] Reiss H, Frisch HL, Lebowitz JL. J Chem Phys 1959;31:369.
[34] Kowert BA, Dang NC, Sobush KT, Seele III LG. J Phys Chem A 2001;105:1232.
[35] Kowert BA, Dang NC, Reed JP, Sobush KT, Seele III LG. J Phys Chem A 2000;104:8823.
[36] Bicerano J. Prediction of polymer properties, 2nd ed. New York: Marcel Dekker; 1996.
[37] Takeuchi H, Okazaki K. J Chem Phys 1990;92:5643. Takeuchi H, Roe RJ, Mark JE. J Chem Phys 1990;93:9042.
[38] Bharadwaj RK, Boyd RH. Polymer 1999;40:4229.
[39] Sok RM, Berendsen HJC, van Gunsteren WF. J Chem Phys 1992;96:4699.
[40] Gusev AA, Arizzi S, Suter UW, Moll DJ. J Chem Phys 1993;99:2221. Gussev AA, Suter UW. J Chem Phys 1993;99:2228.
[41] Sonnenburg J, Gao J, Weiner JH. Macromolecules 1990;23:4653.
[42] Weber H, Paul W. Phys Rev E 1996;54:3999.
[43] Takeuchi H. J Chem Phys 1990;93:2062.
[44] Shah VM, Stern SA, Ludovice PJ. Macromolecules 1989;22:4660.
[45] Pant PVK, Boyd RH. Macromolecules 1993;26:679.
[46] Park HS, Chang T, Lee SH. J Chem Phys 2000;113:5502.